

Static Potential in the SU(2)-Higgs Model and Coupling Constant Definitions in Lattice and Continuum Models

F. Csikor, Z. Fodor, P. Hegedüs, A. Piróth
*Institute for Theoretical Physics, Eötvös University,
H-1088 Budapest, Hungary*

Abstract

We present a one-loop calculation of the static potential in the SU(2)-Higgs model. The connection to the coupling constant definition used in lattice simulations is clarified. The consequences in comparing lattice simulations and perturbative results for finite temperature applications are explored.

PACS Numbers: 11.15.Ha, 12.15.-y

1 Introduction

The observed baryon asymmetry of the universe was eventually determined at the electroweak phase transition [1]. The most straightforward method to study this phase transition is to use resummed perturbation theory (cf. e.g. [2, 3, 4]). In the low temperature Higgs phase the perturbative approach is expected to work well, however, it is not able to describe the high temperature symmetric phase, which has serious infrared problems in perturbation theory. Since the determination of thermodynamical quantities at the critical temperatures is based on the properties of both phases, non-perturbative techniques are necessary for a quantitative understanding of the phase transition.

One very successful possibility is to construct an effective 3-dimensional theory by using dimensional reduction, which is a perturbative step. The non-perturbative study is carried out in this effective 3-dimensional model (see e.g. [5] and references therein). Analytical estimates are confirmed by numerical results and relative errors are believed to be at the percent level.

Another approach is to use 4-dimensional simulations. The complete lattice analysis of the Standard Model is not feasible due to the presence of chiral fermions, however, the infrared problems are connected only with the bosonic sector. These are the reasons why the problem is usually studied by simulating the SU(2)-Higgs model on 4-dimensional lattices, and perturbative steps are used to include the U(1) gauge group and the fermions. Finite temperature simulations are carried out on lattices with volumes $L_t \cdot L_s^3$, where $L_t \ll L_s$ are the temporal and spatial extensions of the lattice, respectively. The lattice spacing is basically fixed by the number of the lattice points in the

temporal direction ($T_c = 1/(L_t a)$, where T_c is the critical temperature in physical units); therefore huge lattices are needed to study the soft modes. This problem is particularly severe for Higgs boson masses around the W mass, for which the phase transition is weak and typical correlation lengths are much larger than the lattice spacing. In this case asymmetric lattice spacings are used, in particular the spatial lattice unit is approximately four times larger than the temporal one [6].

Despite the fact that the two approaches (perturbative and lattice) are systematic and well-defined, it is not easy to compare their predictions. The reason for this is that in lattice simulations the gauge coupling constant is determined from the static potential, whereas in perturbation theory the $\overline{\text{MS}}$ scheme is used. The main goal of this paper is to perform as perfect a comparison as possible, by determining the $\overline{\text{MS}}$ gauge coupling constants, which correspond to the different lattice results.¹

The paper is organized as follows. Section 2 contains the one-loop static potential of the SU(2)-Higgs model using the $\overline{\text{MS}}$ scheme in the Feynman gauge. Section 3 relates the continuum version of the lattice gauge coupling constant to the $\overline{\text{MS}}$ coupling. In Section 4 the detailed comparison of lattice and perturbative predictions are presented. Section 5 summarizes our results.

2 Calculation of the one-loop static potential

The one-loop static potential was calculated long ago in quantum chromodynamics [8, 9, 10], and even the full two-loop result was published recently [11]. The calculation is based on the same principles and techniques in the case of the SU(2)-Higgs model. One calculates rectangular Wilson loops of size $r \times t$. The logarithm divided by $-t$ gives the potential at distance r in the $t \rightarrow \infty$ limit.

Our calculation was performed in the $\overline{\text{MS}}$ scheme and the Feynman gauge but the result is gauge independent, as it should be for a physical observable. The relevant graphs are shown in Fig. 1. Other graphs, giving vanishing contributions in the Feynman gauge and are not shown in Fig. 1. Solid lines represent the heavy quark (antiquark) propagator, while wavy lines the vector boson propagator. External heavy quark (antiquark) propagators are not shown in the figure. The one-loop corrected vector boson propagator contains scalar and ghost contributions as well. The result can be conveniently given in momentum space. One obtains

$$\begin{aligned}
V_{1\text{-loop}}(k) = & -\frac{3g^4}{32\pi^2} \frac{1}{k^2 + M_W^2} \\
& \left\{ \frac{k^2 + M_W^2}{k} \frac{2}{\sqrt{k^2 + 4M_W^2}} \log \frac{\sqrt{k^2 + 4M_W^2} - k}{\sqrt{k^2 + 4M_W^2} + k} \right. \\
& + \frac{1}{k^2 + M_W^2} \left[\frac{1}{24R_{HW}^2} (86R_{HW}^2 k^2 - 9(6 - 3R_{HW}^2 + R_{HW}^4)M_W^2) \log \frac{\mu^2}{M_W^2} \right. \\
& \quad \left. + \frac{1}{8}(13k^2 - 20M_W^2)F(k^2; M_W^2, M_W^2) \right. \\
& \quad \left. - \frac{1}{24} \left((R_{HW}^2 - 1)^2 \frac{M_W^4}{k^2} + k^2 + 2(R_{HW}^2 - 5)M_W^2 \right) F(k^2; M_W^2, M_H^2) \right. \\
& \quad \left. + \frac{R_{HW}^2 \cdot \log R_{HW}}{12(R_{HW}^2 - 1)} (k^2 + (9R_{HW}^2 - 17)M_W^2) \right.
\end{aligned}$$

¹ During the write-up of our results, prior to us, a similar, independent calculation for the gauge coupling constant was presented by M. Laine [7], who compared 4-dimensional and 3-dimensional results, too. Using his convention for the renormalized gauge coupling, which is a special case of our definition, the two results agree. However, as it will be discussed later, our definition for the perturbative gauge couplings is closer to the actual lattice definitions.

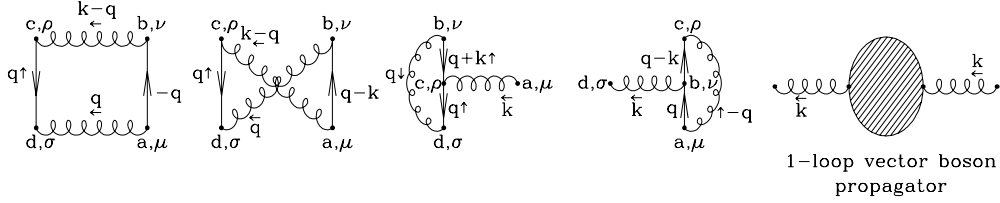


Figure 1: Graphs giving nonvanishing contributions to the static potential

$$+ \frac{1}{72R_{HW}^2} \left(R_{HW}^2 k^2 + 3(-18 + R_{HW}^2 - 11R_{HW}^4)M_W^2 \right) \Bigg\}, \quad (1)$$

where k^2 denotes the square of the three-momentum \vec{k} , M_H the Higgs mass and $R_{HW} = M_H/M_W$. The function F is defined as

$$F(k^2; m_1^2, m_2^2) = 1 + \frac{m_1^2 + m_2^2}{m_1^2 - m_2^2} \log \frac{m_1}{m_2} + \frac{m_1^2 - m_2^2}{k^2} \log \frac{m_1}{m_2} + \frac{1}{k^2} \sqrt{(m_1 + m_2)^2 + k^2} ((m_1 - m_2)^2 + k^2) \log \frac{1 - \sqrt{\frac{(m_1 - m_2)^2 + k^2}{(m_1 + m_2)^2 + k^2}}}{1 + \sqrt{\frac{(m_1 - m_2)^2 + k^2}{(m_1 + m_2)^2 + k^2}}}. \quad (2)$$

As it can be seen, our result does depend on the renormalization scale μ and it fully agrees with that of M. Laine [7].

Eq. (1) has to be Fourier transformed into coordinate space. We applied the brute force method performing numerical integration. As a check, we compared our results with various pieces of the partly analytic calculation in [7] for the derivative of the potential (with respect to distance). The agreement is excellent.

Our result is presented in Figs. 2 and 3, where the various parts of the one-loop correction to the potential are plotted. We define

$$\frac{V(r)}{M_W} = -\frac{3g^2}{16\pi} \frac{\exp(-M_W^0 r)}{M_W r} + \frac{g^4}{16\pi^2} \left(A + B \log(\mu^2/M_W^2) \right), \quad (3)$$

where $M_W^0 = M_W - \delta M_W$, with δM_W the one-loop mass correction. Since δM_W is scale dependent, so is M_W^0 . A and B are functions of the distance r and $R_{HW} = M_H/M_W$. We choose $M_W = 80\text{GeV}$. Fig. 2 shows the dependence of A and B on the dimensionless distance rM_W for $R_{HW} = 0.8314$ (corresponding to the end point of the first order finite temperature phase transition [12]), while Fig. 3 shows the R_{HW} dependence for $r = M_W^{-1}$.

3 Relation of the continuum version of the lattice coupling constant definition to the $\overline{\text{MS}}$ coupling constant

Since we wish to compare results of lattice simulations and continuum perturbation theory calculations, it is an essential point to define the $\text{SU}(2)$ gauge coupling in the same way in both cases. However, in continuum perturbation theory the $\overline{\text{MS}}$ running coupling constant at a given renormalization scale is more natural (as used in Eqs. (1,3), too), while in lattice simulations other definitions are applied. Therefore we have to establish the relation between the coupling constants.

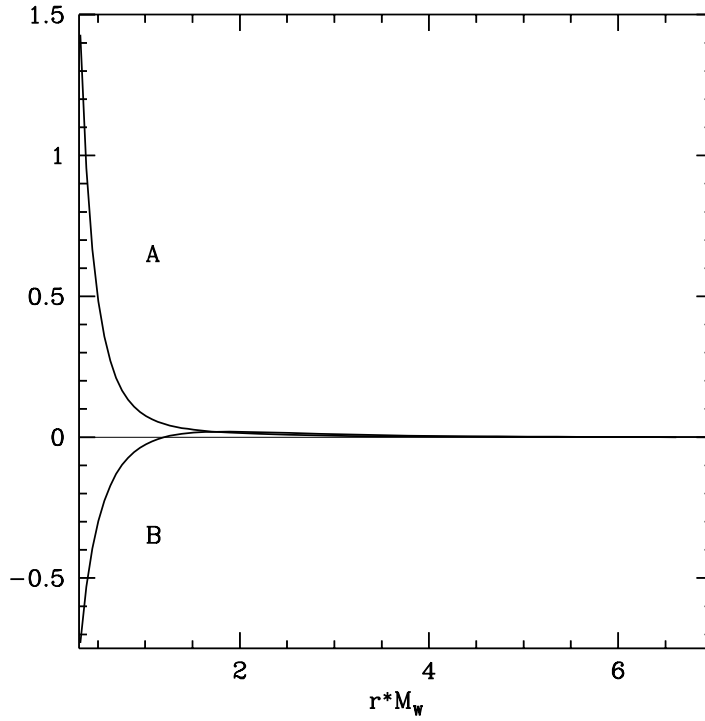


Figure 2: The coefficients of $g^4/(16\pi^2)$ —curve A—and of $g^4/(16\pi^2) \log(\mu^2/M_W^2)$ —curve B—of the static potential Eq. (3) as a function of distance times W mass. $R_{HW}=0.8314$.

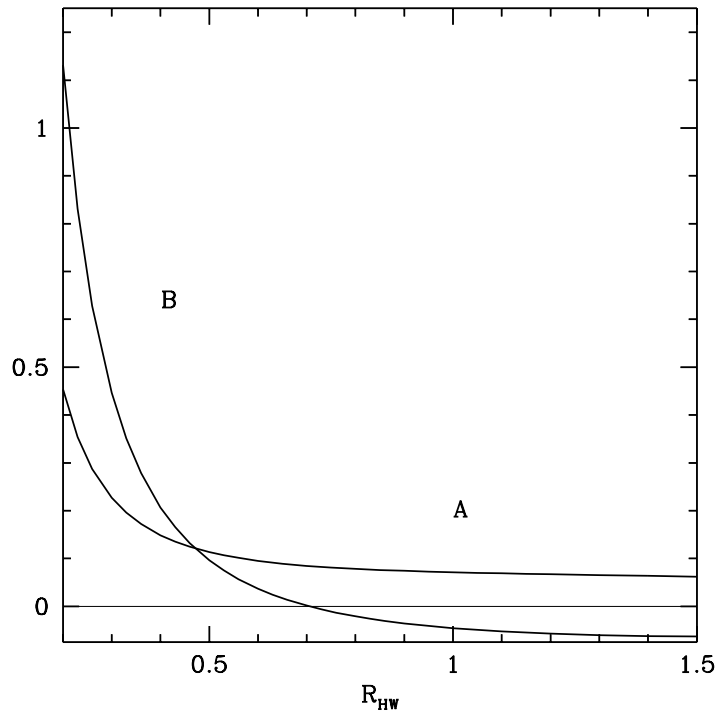


Figure 3: The coefficients of $g^4/(16\pi^2)$ —curve A—and of $g^4/(16\pi^2) \log(\mu^2/M_W^2)$ —curve B—of the static potential Eq. (3) as a function of R_{HW} . The distance is M_W^{-1} .

The lattice definition of the coupling constant is given in [13]. Note that we are using the local version below. For the reader's convenience we recall this definition (inspired by [14]).

First rectangular Wilson loops of size (r,t) are measured. Extrapolating to large t and dividing the logarithm by $-t$ one gets the static potential in the $t \rightarrow \infty$ limit as a function of r . The nonperturbative lattice static potential is fitted by a finite lattice version of the Yukawa potential with four parameters (for details cf. [13]). One of these parameters is the mass in the exponential of the Yukawa potential, which is usually called the screening mass. The gauge coupling at distance r is defined as the ratio of the discrete r derivative of the lattice simulated nonperturbative potential and the discrete derivative of the tree-level lattice Yukawa potential normalized by the square of the tree-level coupling and with the mass parameter M_{lattice} identified with the screening mass. In practice $g_{\text{lattice}}^2(M_{\text{lattice}}^{-1})$ is determined and is called the local renormalized gauge coupling constant on the lattice. The lattice results at various Higgs masses are collected in Table 1. Data are from [6],[12],[13], and [15].

To follow the above procedure in the case of the continuum perturbative determination of the renormalized gauge coupling, we performed a fit of the one-loop potential with a tree-level Yukawa potential plus a constant term. The parameters of the fit are the coupling constant, the mass in the exponent (perturbative "screening mass" M_{screen}) and the constant. For the various values of Higgs mass we performed the fit in the same r range as used in the lattice studies and took the errors of the fitted function to be proportional to the errors of the potential obtained in lattice simulations. $g_R^2(r)$ is then determined by taking the ratio of the derivatives with respect to r of the one-loop potential and the tree-level potential normalized by the square of the tree-level coupling, i.e. we have

$$g_R^2(r) = \frac{1}{C_F} \frac{\frac{d}{dr} [-V(r)]}{\frac{d}{dr} \int \frac{d^3k}{(2\pi)^3} \frac{\exp(i\vec{k} \cdot \vec{r})}{k^2 + M_{\text{screen}}^2}}, \quad (4)$$

with $V(r)$ given by Eq. (3), $C_F = 3/4$, and M_{screen} obtained from the fit. Since $M_{\text{screen}} - M_W^0 = O(g^2)$, for distances satisfying $M_{\text{screen}} - 1/r = O(g^2)$ we can put Eq. (4) into the form

$$g_R^2(r) = g_{\overline{\text{MS}}}^2(\mu) \left(1 + \frac{1}{2} \left(1 - \frac{M_W^0}{M_{\text{screen}}} \right) \right) + \frac{g_{\overline{\text{MS}}}^4(\mu)}{16\pi^2} \left(C + D \log \frac{\mu^2}{M_W^2} \right). \quad (5)$$

C and D are functions of R_{HW} and M_{screen} , their values are tabulated in Table 2 for $M_{\text{screen}} = M_W = 80\text{GeV}$.

R_{HW}	.2049	.4220	.595	.8314
T_c (GeV)	38.3	72.6	100.0	128.4
M_{lattice} (GeV)	84.3(12)	78.6(2)	80.0(4)	76.7(24)
$g_{\text{lattice}}^2(M^{-1})$.5630(60)	.5788(16)	.5782(25)	.569(4)
M_{screen} (GeV)	74.97	80.44	80.70	81.77
$g_{\overline{\text{MS}}}^2(T_c)$	0.540	0.592	0.585	0.570
$g_{\overline{\text{MS}}}^{2,Laine}(T_c)$	0.589	0.589	0.579	0.562

Table 1: Various quantities calculated for values of R_{HW} used in lattice simulations. For more explanation see the text. As usual the numbers in the parentheses denote the errors in units of the last decimals. The errors of the different gauge couplings are dominated by the lattice simulation errors (fourth row), therefore we did not indicate them in rows 6 and 7.

In this procedure we have to choose the gauge coupling in the one-loop potential so that $g_R^2(M_{\text{screen}}^{-1})$ reproduces the lattice result (third row of Table 1) for the appropriate value of the Higgs mass. For our applications (thermodynamical quantities at and around the critical temperature T_c of the first order electroweak phase transition) the scale of the one-loop potential is chosen to be $T_c \approx 2M_H$, where M_H is the Higgs boson mass at zero temperature. Thus the gauge coupling appearing in the one-loop potential is actually the $\overline{\text{MS}}$ gauge coupling at scale T_c . The $\overline{\text{MS}}$ gauge coupling values obtained from this procedure are given in the sixth row of Table 1.

Another definition of the continuum perturbation theory one-loop “renormalized gauge coupling” at distance r is given in [7]. It reads

$$g_{R,Laine}^2(r) = \frac{1}{C_F} \frac{\frac{d}{dr} [-V(r)]}{\frac{d}{dr} \int \frac{d^3k}{(2\pi)^3} \frac{\exp(i\vec{k} \cdot \vec{r})}{k^2 + M^2}}, \quad (6)$$

where M is a free mass parameter satisfying $M - M_W \propto g^2$. For this M it is possible to show that $g_{R,Laine}^2(M^{-1})$ can be expressed in terms of $g_{\overline{\text{MS}}}^2(M_W)$, (where M_W is the physical (one-loop) pole mass) and all the scale dependence is included in $g_{\overline{\text{MS}}}^2(M_W)$. Assuming $M = M_W$, the numerical difference between this definition and ours is small. However, we believe that it is our definition which is the closest conceivable to the local renormalized lattice gauge coupling of [13]. In Table 1 (last row) we give $g_{\overline{\text{MS}}}^{2,Laine}(T_c)$ as calculated using Eq. (6), equating $g_{R,Laine}^2(M_W^{-1})$ with the values of the lattice simulation results $g_{\text{lattice}}^2(M_{\text{lattice}}^{-1})$ and using the renormalization group equation to extrapolate to the scale T_c .

R_{HW}	C	D
0.2	-41.54	-22.19
0.3	-8.26	-6.58
0.4	-6.47	-1.12
0.5	-5.66	1.39
0.6	-5.23	2.74
0.7	-4.98	3.55
0.8	-4.83	4.06
0.9	-4.72	4.39
1.0	-4.65	4.62
1.1	-4.59	4.78
1.2	-4.54	4.89
1.3	-4.50	4.98
1.4	-4.45	4.98
1.5	-4.40	5.01

Table 2: The coefficients C and D defined in Eq. (5) as a function of R_{HW} .

4 Comparison of physical observables determined in lattice simulations with perturbative predictions

In the previous section we presented a calculation connecting the renormalized gauge coupling constant of the $\overline{\text{MS}}$ scheme and g_R^2 obtained from the static potential at different distances. In this

section we compare the lattice results and the perturbative predictions for the finite temperature electroweak phase transition. Lattice Monte Carlo simulations provide a well-defined and systematic approach to study the features of the finite temperature electroweak phase transition. During the last years large scale numerical simulations have been carried out in four dimensions in order to clarify non-perturbative details [6],[12],[13],[15]. Thermodynamical quantities (e.g. critical temperature, jump of the order parameter, interface tension, latent heat) have been determined and extrapolation to the continuum limit has been performed in several cases. Nevertheless, it has proven difficult to compare the perturbative and the lattice results, because the perturbative approach used the $\overline{\text{MS}}$ scheme for the gauge coupling, whereas the lattice determination of the gauge coupling has been based on the static potential. The main reason for performing the one-loop calculation of the static potential is this kind of comparison.

In this paper we use the published perturbative two-loop result for the finite temperature effective potential of the SU(2)-Higgs model [4]. Note that the numerical evaluation of the one-loop temperature integrals gives a result which agrees with the approximation based on high temperature expansion within a few percent. The reason for this is that the perturbative expansion up to order g^4, λ^2 corresponds to a high temperature expansion, which is quite precise for the Higgs boson masses we studied. It is known that the perturbative loop expansion becomes unreliable for Higgs masses above approximately 50 GeV (e.g. resummed perturbation theory fails to predict the end-point of the electroweak phase transition, thus it gives a first order phase transition for arbitrarily large Higgs boson masses). In the physically relevant range of the parameter space the electroweak phase transition can only be understood by means of non-perturbative methods. Therefore it is particularly instructive to see quantitatively how the perturbative and the lattice results agree for small Higgs boson masses and how they differ for larger ones.

Since the finite temperature electroweak phase transition is fairly strong for Higgs boson masses below 50 GeV, lattices with symmetric lattice spacings were used for $M_H \approx 16$ GeV, $M_H \approx 34$ GeV and $M_H \approx 48$ GeV. The phase transition gets weaker for larger Higgs boson masses, therefore Monte Carlo simulations for masses near the W-boson mass are technically difficult. For this parameter region different lattice spacings were used in the temporal and the spatial directions. For this type of lattice regularization the approach to the continuum limit is somewhat slower; however, even in this case it was possible to perform a continuum limit extrapolation for $M_H \approx 67$ GeV.

In lattice simulations the gauge coupling constant are determined from the static potential, whereas masses are extracted from correlation functions. On the one hand the calculation of the previous section connects the gauge coupling definitions between the $\overline{\text{MS}}$ scheme and the scheme based on the static potential. On the other hand one can use the zero temperature effective potential in order to include the most important mass renormalization effects. The Higgs boson mass obtained from the asymptotics of the correlation function corresponds to the physical mass determined by the pole of the propagators, i.e. the solution of $p^2 - M^2 = \Pi(p^2)$, where $\Pi(p^2)$ is the self-energy. The effective potential approach suggested by Arnold and Espinosa [2] approximates $\Pi(p^2)$ by $\Pi(0)$ in the above dispersion relation. It has been argued that the difference between the two expressions is of order $g^5 v^2$ (v is the zero-temperature vacuum expectation value), which does not affect our discussion. In this scheme the correction to the $\overline{\text{MS}}$ potential reads

$$\delta V = \frac{\varphi^2}{2} \left(\delta m^2 + \frac{1}{2\beta^2} \delta \lambda \right) + \frac{\delta \lambda}{4} \varphi^4, \quad (7)$$

where

$$\delta m^2 = \frac{9g^4 v^2}{256\pi^2}, \quad \delta \lambda = -\frac{9g^4}{256\pi^2} \left(\log \frac{M_W^2}{\mu} + \frac{2}{3} \right). \quad (8)$$

Here μ is the renormalization scale and M_W is the W-boson mass at $T = 0$. The above notation corresponds to a tree-level potential of the form $m^2 \varphi^2/2 + \lambda \varphi^4/4$. Note that this treatment is

M_H		16.4(7)	33.7(10)	47.6(16)	66.5(14)
g_R^2		0.561(6)	0.585(9)	0.585(7)	0.582(7)
T_c/M_H	pert	2.72(3)	2.28(1)	2.15(2)	1.99(2)
	nonpert	2.34(5)	2.15(4)	2.10(5)	1.93(7)
φ_+/T_c	pert	4.30(23)	1.58(7)	0.97(4)	0.65(2)
	nonpert	4.53(26)	1.65(14)	1.00(6)	0
Q/T_c^4	pert	0.97(7)	0.22(2)	0.092(6)	0.045(2)
	nonpert	1.57(37)	0.24(3)*	0.12(2)	0
σ/T_c^3	pert	0.70(10)	0.067(6)	0.022(2)	0.0096(5)
	nonpert	0.77(11)	0.053(5)*	0.008(2)*	0

Table 3: Comparison of the perturbative and the lattice results. The Monte Carlo data are from [6],[12],[13],[15] (in some cases we have refined the analysis in order to have a more accurate lattice prediction). Note that for the mass of the W boson—the dimensionful quantity setting the scale of the theory—80 GeV is used.

analogous to previous comparisons of the perturbative and lattice results [16].

In [6],[12],[13],[15] several observables were determined, including renormalized masses at zero temperature (M_H , M_W), critical temperatures (T_c), jumps of the order parameter (φ_+), latent heats (Q) and surface tensions (σ) for different Higgs boson masses. As usual, the dimensionful quantities were normalized by the proper power of the critical temperature. (This convention is adapted in the present paper, too.) The simulations were performed on $L_t = 2, 3, 4, 5$ lattices (L_t is the temporal extension of the finite-temperature lattice) and whenever it was possible a systematic continuum limit extrapolation was carried out assuming standard $1/a^2$ corrections for the bosonic theory.

The statistical errors of these observables are normally determined by comparing statistically independent samples. Jackknife and bootstrap techniques were used [17] and correlated fits were performed [18] to obtain reliable estimates of the statistical uncertainties. The systematic errors due to finite lattice spacing can be obtained by $1/a^2$ extrapolation. In cases where it was possible to carry out the continuum limit extrapolation we saw that the difference between the $L_t = 2$ and the $L_t = 3$ data was a fairly good estimator of the systematic error. Whenever the data did not make it possible to carry out the systematic extrapolation the difference between the $L_t = 2$ and the $L_t = 3$ results was used to estimate the systematic error. As a conservative estimate we added the statistical and systematic errors linearly. For some of the quantities only $L_t = 2$ data exist. In these cases only the statistical errors are listed and an asterisk is used in Table 3 as an indication. A correct comparison has to include errors on the parameters used in the perturbative calculation. These uncertainties are connected with the fact that neither the Higgs boson mass nor the gauge coupling constant can be determined exactly in lattice simulations. Including these errors, the perturbative prediction for an observable is rather an interval than one definite value.

To obtain a better measure of the correspondence between perturbative and nonperturbative results, and to incorporate their errors, one introduces “pulls” defined by the expression

$$\text{pull} = \frac{\text{perturbative mean} - \text{nonperturbative mean}}{\text{perturbative error} + \text{nonperturbative error}}. \quad (9)$$

The four different pulls at different Higgs boson masses are tabulated in Table 4 and plotted in Fig. 4. For the sake of convenience, we used the shorthand $P_T = \text{pull of } T_C/M_H$, $P_\phi = \text{pull of } \varphi_+/T_C$, $P_Q = \text{pull of } Q/T_C^4$, and $P_\sigma = \text{pull of } \sigma/T_C^3$.

The quantity which has the smallest pull even for large Higgs boson masses is T_c/M_H . A quadratic

m_H (GeV)	16.4(7)	33.7(10)	47.6(16)	66.5(14)
P_T	4.75	2.60	0.71	0.67
P_ϕ	0.47	-0.33	-0.3	32.5
P_Q	-1.36	-0.4	-1.08	22.5
P_σ	-0.33	1.27	3.5	19.2

Table 4: Values of the four different pulls for various Higgs boson masses

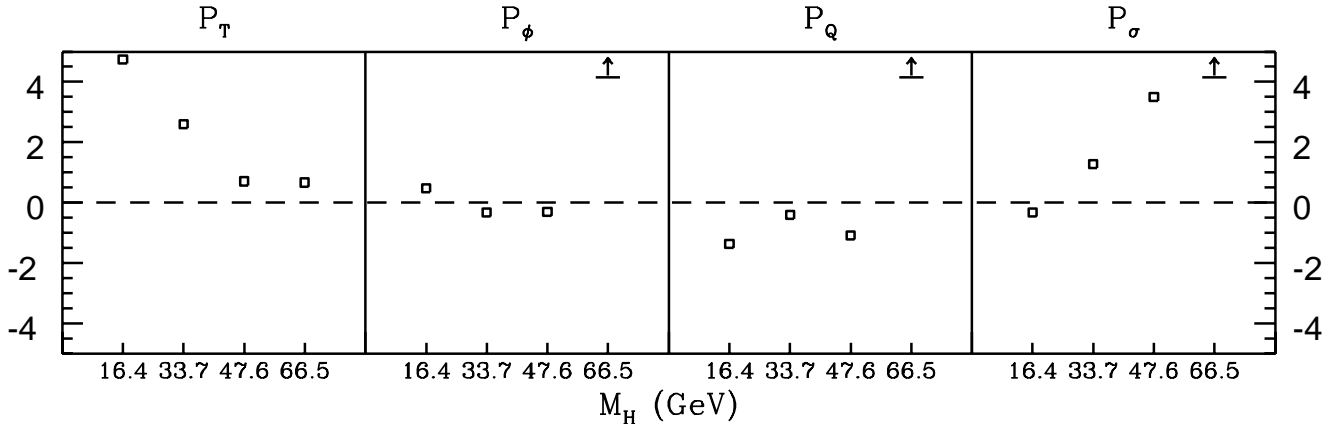


Figure 4: “Pulls” plotted against the Higgs mass. Arrows indicate values outside the interval $[-5, 5]$.

fit was performed to this quantity as a function of R_{HW} . The result is

$$\frac{T_c}{M_H} = 2.494 - 0.842R_{HW} + 0.223R_{HW}^2. \quad (10)$$

In [12] the end point result for the four-dimensional SU(2)-Higgs model was perturbatively converted to the Standard Model. In this step the deviation between the two definitions of the gauge coupling ($g_{\overline{\text{MS}}}^2$ and the one based on the static potential) was neglected. The estimated uncertainty due to this simplification was included into the systematic error of the end point Higgs mass. Using the results of the present paper we can also refine the value of the Standard Model end point Higgs mass. This is done by perturbatively taking into account fermions and the U(1) factor of the Standard Model (for details see the fourth paper of [5]). The improvement is established by precisely converting the lattice simulation renormalized gauge coupling of the SU(2)-Higgs model into the perturbative $g_{\overline{\text{MS}}}^2(M_W)$. The new value of the Standard Model end point Higgs mass is $72.1 \pm 1.4\text{GeV}$. This does not deviate much from the old value $72.4 \pm 1.7\text{GeV}$ of [12]. However, the error is smaller, since the uncertainty arising from the gauge coupling definitions is eliminated.

5 Summary

In this paper we presented the one-loop static potential in the SU(2)-Higgs model. This calculation is in agreement with [7]. Using the potential it was possible to connect the gauge coupling constant used in finite temperature field theory and in lattice simulations. As expected the numerical difference between the two conventions is not that large, it is within a few percent. With this connection

we were able to perform a precise comparison between the predictions of perturbative and lattice approaches.

We reanalyzed the existing lattice data and performed a continuum limit extrapolation whenever it was possible. The relationship between the two definitions of the gauge coupling constants turned out to be marginal, as the lattice data have errors, usually larger than this few percent. The only quantity which is measured so precisely that the definition of the gauge coupling constant is essential is the ratio of the critical temperature to the Higgs boson mass. As it has been observed already for $M_H \approx 35$ GeV the perturbative value of T_c is larger than in lattice simulations. This sort of discrepancy disappears for larger Higgs boson masses. A plausible reason for this fact is the convergence of the high temperature expansion used in the perturbative approach. In two-loop perturbation theory one uses the high temperature expansion also up to second order, which might be inaccurate for the smallest Higgs mass case with temperatures ≈ 50 GeV and Higgs field expectation values ≈ 200 GeV. Nevertheless, the observed differences are on the percent level and they do not affect the electroweak phase transition significantly. For small Higgs boson masses (16 and 34 GeV) we expect similar differences between lattice and perturbative predictions for other quantities (the jump of the order parameter, the latent heat and the surface tension); however, present lattice data have too large errors and the differences cannot be seen yet.

The most dramatic differences appear clearly as we get closer to the end point. The perturbative approach gives nonvanishing jump of the order parameter, nonvanishing latent heat and interface tension, while the lattice results suggest rapid decrease of these quantities and no phase transition beyond the end point.

Using the results of the present paper we refined the value of the Standard Model end point Higgs mass of [12] and obtained 72.1 ± 1.4 GeV.

This work was partially supported by Hungarian Science Foundation Grants under Contract No. OTKA-T22929-29803-M28413/FKFP-0128/1997.

References

- [1] V. A. Kuzmin, V. A. Rubakov and M. E. Shaposhnikov, Phys. Lett. **B155** 36 (1985).
- [2] P. Arnold and O. Espinosa, Phys. Rev. **D47** 3546 (1993), Erratum ibid. **D50** 6662 (1994).
- [3] W. Buchmüller et al., Ann. Phys. (NY) **234** 260 (1994).
- [4] Z. Fodor and A. Hebecker, Nucl. Phys. **B432** 127 (1994).
- [5] K. Farakos et al., Nucl. Phys. **B425** 67 (1994);
A. Jakovác, K. Kajantie and A. Patkós, Phys. Rev. **D49** 6810 (1994);
A. Jakovác and A. Patkós, Nucl. Phys. **B494** 54 (1997);
K. Kajantie et al., Nucl. Phys. **B458** 90 (1996); ibid. **B466** 189 (1996); ibid. **B493** 413 (1997);
Phys. Lett. **B423** 137 (1998); Phys. Rev. Lett. **77** 2887 (1996);
F. Karsch et al., Nucl. Phys. Proc. Suppl. **53** 623 (1997);
M. Gürtler et al., Phys. Rev. **D56** 3888 (1997); E.-M. Ilgenfritz et al., Eur. Phys. J. **C8** 135 (1999);
K. Rummukainen et al., Nucl. Phys. **B532** 283 (1998);
- [6] F. Csikor and Z. Fodor, Phys. Lett. **B380** 113 (1996);
F. Csikor, Z. Fodor and J. Heitger, Phys. Rev. **D58** 094504 (1998).
- [7] M. Laine, hep-ph/9903513 (1999)
- [8] L. Susskind, Coarse Grained Quantum Chromodynamics in R. Balian and C. H. Llewellyn Smith (eds.), Weak and Electromagnetic Interactions at High Energy (North Holland, Amsterdam, 1977).
- [9] W. Fishler, Nucl. Phys. **B129** 157 (1977).
- [10] T. Appelquist, M. Dine and I. L. Muzinich, Phys. Lett. **B69** 231 (1977).
- [11] M. Peter, Phys. Rev. Lett. **78** 602 (1997); Nucl. Phys. **B501** 471, (1997);
Y. Schröder, Phys. Lett. **B447** 321 (1999).
- [12] F. Csikor, Z. Fodor and J. Heitger, Phys. Rev. Lett. **82** 21 (1999).
- [13] Z. Fodor et al., Phys. Lett. **B334** 405 (1994);
Z. Fodor et al., Nucl. Phys. **B439** 147 (1995).
- [14] R. Sommer, Nucl. Phys. **B441** 839 (1994).
- [15] F. Csikor et al., Nucl. Phys. **B474** 421 (1996); F. Csikor et al., Phys. Lett. **B357** 156 (1995);
J. Hein and J. Heitger, Phys. Lett. **B385** 242 (1996); Y. Aoki, Phys. Rev. **D56** 3860 (1997);
F. Csikor, Z. Fodor and J. Heitger, Phys. Lett. **B441** 354 (1999); Y. Aoki et al., Phys. Rev. **D60** 013001 (1999).
- [16] W. Buchmüller, Z. Fodor and A. Hebecker, Nucl. Phys. **B447** 317 (1995).
- [17] B. Efron, SIAM Review **21** 460 (1979);
R. Gupta et al., Phys. Rev. **D36** 2813 (1987).
- [18] C. Michael and A. McKerrell, Phys. Rev. **D51** 3745 (1995).